Journal of Applied Polymer Science

Fabrication and improved performance of poly(3-hydroxybutyrate-co-3-hydroxyvalerate) for packaging by addition of high molecular weight natural rubber

Sunny J. Modi,[1] Katrina Cornish,[2] Kurt Koelling,[3] Yael Vodovotz[1]

[1]Department of Food Science and Technology, Ohio State University, 110 Parker Food Science and Technology Bldg, 2015 Fyffe Road, Columbus, Ohio, 43210

[2]Department of Horticulture and Crop Science, Department of Food Agricultural and Biological Engineering, Ohio State University, 1680 Madison Avenue, Wooster, Ohio, 44691

[3]Department of Chemical and Biomolecular Engineering, Ohio State University, 125 Koffolt Laboratories, 140 West 19th Avenue, Columbus, Ohio, 43210

Correspondence to: Y. Vodovotz (E-mail: vodovotz.1@osu.edu)

ABSTRACT: The packaging industry is searching for alternative materials to attain environmental sustainability. Poly(3-hydroxybutyrate-co-3-hydroxyvalerate (PHBV) is a semicrystalline polymer that meets this sustainability goal since it is bioderived and biodegradable. However, its brittle nature and relatively high water permeation and transmission rates make it unsuitable for packaging applications. In addition, PHBV has poor mechanical, thermal, and rheological properties above 160 °C, limiting its use in cast sheets and thermo-formed packaging applications. To improve these properties, new blends of PHBV with high molecular weight natural rubber at 5, 10, 15, and 25% by weight were fabricated, and physico-chemical properties of the blends were characterized. The rubber in the blends aided in the following: increased thermal stability since the complex viscosities of the blends were improved by one log over pure PHBV at 170 °C, created more uniform melting peaks attesting to improved homogeneity, decreased water permeation to a level similar to that of traditional thermoplastics; increased the elongation at break, and stabilized the Young's modulus. Therefore, these blends can potentially be used in-place of traditional, petroleum-based thermoplastics in cast sheets and thermoforms. © 2016 Wiley Periodicals, Inc. J. Appl. Polym. Sci. **2016**, *133*, 43937.

KEYWORDS: biomaterials; biopolymers and renewable polymers; blends; rubber

Received 3 December 2015; accepted 16 May 2016
DOI: 10.1002/app.43937

INTRODUCTION

In the current economy, there is an increasing need for packaging materials for safe and efficient distribution of goods. To address this need, the global plastics industry has grown 9% annually over the last decade and is expected to continue to grow at a similar rate.[1] Currently, these plastic materials are derived from petroleum-based feedstocks that are not compostable, contribute to environmental pollution, and threaten the habitats of many animals.[2] In addition, the amount of plastic being discarded continues to increase.[2,3] According to Plastic Europe and United States Environmental Protection Agency, in 2012, Europe released 25.2 million tons of plastics into waste streams, while the United States contributed 31.9 million tons.[1,4] The current green movement to increase recyclable plastics has generated some lower quality materials due to cross contamination of different polymers or comingled waste streams. Incineration of plastic waste produces carbon dioxide and other toxic gases that spill into the environment during combustion.[2] It is very difficult to reduce the consumption of plastic products due to their versatile properties, but it is possible to develop sustainable replacement materials with equivalent functionality and properties.

Bacteria and enzymes can degrade aliphatic polymers with hydrolyzable carbon backbones, such as bacterially synthesized poly(3-hydroxybutyrate) (PHB), thus alleviating landfill saturation.[5–8] PHB is produced by nutrient-deprived microorganisms, which accumulate the polymer as an intracellular form of energy storage.[4–9] However, commercial use of PHB is limited due to thermal degradation, and brittleness at room temperature,[4–9] in addition to its higher production costs. During the growth stage of PHB homopolymer, incorporation of propionic or pentanoic acid, while restricting dissolved oxygen, leads to

the formation of 3-hydroxyvalerate (PHV). PHBV, although a promising bioplastic, has poor thermal and mechanical properties above 160 °C.[10–12] Additionally, high processing temperatures within the extruder resulted in thermal degradation of the polymer near or above the melting temperature (171 °C) of the PHBV.[10]

Hevea brasiliensis [the para rubber tree is a source of natural rubber (NR)], elastomer with high elasticity and yield strength. NR is obtained as latex tapped from the laticiferous vessels of *Hevea*.[13] R is a *cis*−1,4-polyisoprene hydrocarbon polymer constructed of isoprene units, and is produced as a secondary metabolic end-product.[14] NR provides an unmatched combination of tensile strength, elasticity, memory, and softness. The high yield strength is due to NR's ability to undergo stress–strain crystallization giving it high tensile strength in the direction of elongation.[14] This produces a superior form of reinforcement as it limits movements between neighboring molecular chains and leads to high ultimate strength.[15,16] The incorporation of dispersed rubber particles into a brittle PHBV thermoplastic matrix is known to improve both the impact resistance and toughness properties with minor decreases in modulus.[15,16] However, these studies incorporated the rubber as a particulate filler. NR polymers have not been blended with PHBV to form a visually uniform blended material.

Recent studies of PHB with rubber have shown marked improvements in their physical properties. PHB composites with poly(epichlorohydrin), poly(ethylene oxide), and poly(vinylacetate), epoxidized NR, and maleated poly-butadiene showed a single glass transition temperature, "drastic depression of equilibrium melting temperature," and had a homogenous crystalline structure.[17–23] In addition, incorporation of dispersed particles of epoxidized rubber (modified form of NR) into a brittle PHBV thermoplastic matrix improved both impact resistance and toughness with minor decreases in modulus.[18] Addition of ethylene-propylene rubber (EPR) to a PHB matrix, caused significant improvement in elongation at break, as well as improvements in modulus and stress properties due to intermolecular interactions between the ester or the alcohol functional groups on the rubber and the ester groups on the PHB polymer.[17] Attempts to blend NR with PHBV initially failed due the difference in viscosity between the two materials (unpublished data). The viscosity of high molecular weight "gel" fraction of NR is closer to that of PHBV and preliminary results were encouraging.[24] Therefore, the main objective of this work was to fabricate PHBV blended with high molecular weight NR (HMW-NR), and assess the physico-chemical properties of the new materials.

EXPERIMENTAL

Materials and Sample Preparation

Commercially available PHBV with 5% HV content was purchased from Tianan Biologic Material Co. (Ningbo, China). *Hevea brasiliensis* rubber was purchased from CentroTrade LLC. (Wadsworth, OH). The rubber was cut into approximately 2.54 cm^3 cubes and soaked in HPLC grade hexane (Fisher Chemicals, Fairlawn, NJ) for approximately three hrs. The rubber cubes were stirred using a Corning PC-420D stir plate (Tewksbury, MA) at 300 rpm for 2 h, and then at 320 rpm for the last hour. This method dissolved the uncrosslinked (non-gel) rubber, and precipitated latex proteins and impurities, but swelled the partially crosslinked HMW-NR (gel). The dissolved fraction was decanted from the partially crosslinked HMW-NR and the residual hexane was evaporated from the HMW-NR for 24 h at room temperature. The dissolved fraction has commercial application in tank liners which are made from gel-free NR. The weight fraction of the original rubber used was approximately 88%.

The PHBV polymer was vacuum dried for 24 h at 60 °C before being compounded with extracted HMW-NR using a Leistritz ZSE-27 twin-screw extruder (Somerville, NJ) with a reverse compounding profile of 170–140 °C. The extrudates were injection molded into ASTM Type I parts using a Sumitomo SH50M (Norcross, GA) injection molder as outlined in the processing guide by Tianan for thermal behavior and water vapor transmission rate characterization. For rheological testing, the extrudates were compression molded into disks (25.0 mm in diameter and approximately 1.0 mm thickness) using a Carver press (Wabash, IN) at 183 °C.

Differential Scanning Calorimetry (DSC)

Differential scanning calorimetry (DSC) (TA Instruments Q100, New Castle, DE) was used to determine the state of the materials as a function of temperature, using a previously described procedure.[10] Samples were vacuum dried at 60 °C for 24 h prior to any testing and stored in a desiccator during the analysis. The average melting transitions were determined from thermograms obtained by heating 5–10 mg samples from −20 to 200 °C at a rate of 10 °C/min. The samples were allowed to anneal at 200 °C for 3–5 min to remove the thermal history of the polymers, and subsequently cooled to −85 °C at 10 °C/min, held for 3–5 min, and reheated from −85 to 200 °C with a heating rate of 10 °C/min. The reported values are averages of four samples.

Thermogravimetric Analysis (TGA)

Thermogravimetric analysis (TGA) was used to study thermal decomposition properties using a TA Instruments TGA 5000 (New Castle, DE). The samples were heated under nitrogen from room temperature to 500 °C with a heating rate of 20 °C/min. Samples were vacuum dried at 60 °C for 24 h prior to any testing. The summarized results are averages of four samples tested.

Water Vapor Transmission Rate

Impact disks with a thickness of 0.72–0.75 mm were used to determine water vapor transmission rates (WVTR) using a Mocon Permatran-W 3/31 (Minneapolis, MN) according to ASTM F1249-06. The Mocon unit was set to 100% relative humidity (r.h.) by using a wet sponge in each cell. Prior to testing, the instrument was calibrated using the Mocon supplied calibration films at 37.8 °C with a flow rate of 100 cm^3/min. To prevent the infrared detector from being overloaded with water vapor, the sample area was reduced to 5 cm^2 using the aluminum foil supplied by Mocon. The samples were analyzed at 37.8 °C with a flow rate of 100 cm^3/min at 100% r.h. in 30-min cycles. The reported values were obtained after the samples had

reached steady state of 12–16 h. The averages of five trials are reported.

Dynamic Mechanical Analysis (DMA)

The mechanically induced glass transitions of the blends were studied using a TA Instrument Q800 (New Castle, DE) as previously described.[10] The samples were equilibrated at −110 °C and subsequently heated to 150 °C with a heating rate of 5 °C/min. The sample dimensions were approximately 25 × 3.0 × 0.70 mm^3 with amplitude of 15.00 μm, preload of 1*N*, and frequency of 1 Hz, using the tension film clamps. The values presented are averages of four specimens.

Creep and Recovery

The visco-elastic behavior of the blends was investigated using a TA Instrument Q800 (New Castle, DE) with tension film clamps. The samples were vacuum dried at 60 °C for 24 h prior to being cut into 15 × 2.0 × 0.7 mm^3 rectangular shapes. The samples were tested at −25, 0, and 25 °C, and held isothermally for 1 min before testing. The samples were creeped at 5 MPa for 5 min, and then recovered for a subsequent 10 min. The reported mean ± standard deviation (SD) values are averages of at least three samples.

Tensile Properties

Tensile properties were determined according to ASTM D638-08. Prior to any testing, the samples were vacuumed dried for 24 h at 60 °C. The tensile data were obtained using an Instron 5542 with Bluehill v. 2.17 software package (Instron Corp. Norwood, MA). Samples were tested using a crosshead speed of 5 mm/min at 26 °C. The reported mean ± standard deviation (SD) values are averages of at least 10 samples. Statistical analysis was performed using Minitab, version 16.0 (State College, PA) on the mechanical properties. Significant differences (*P*-values < 0.05) in tensile data amongst PHBV and their blends were determined using one way analysis of variance (ANOVA) and Fisher method.

Heat Deflection Temperature (HDT)

Heat induced deflection of the blends was measured using a TA Instrument Q800 (New Castle, DE) series DMA as described in ASTM D648 standard. Rectangular bars (35 × 12 × 3.2 mm^3) were tested using dual cantilever clamps with an applied load of 0.455 MPa. The samples were vacuum dried at 60 °C for 24 h and stored in a desiccator prior to any testing. The blends were heated from 30 to 165 °C with a heating rate of 2 °C/min. The reported mean ± standard deviation (SD) values are averages of at least three samples. In addition, statistical analysis was performed using Minitab, version 16.0 (State College, PA). Significant differences (*P*-values <0.05) in the deflection temperatures amongst PHBV and their blends were determined using one way analyses of variance (ANOVA) and the Fisher method.

Rheological Properties

Rheological behavior of the various samples was obtained using a TA Instrument Ares 2000 rheometer (New Castle, DE), as previously described.[10,12] Samples were vacuum dried at 60 °C for 24 h prior to testing. Rheological experiments were performed in the melting temperature range (160–180 °C) using a 25 mm parallel plate system. Each sample was equilibrated for 5 min before the gap was set to the testing position of approximately 0.9 mm or until the top plate made contact with the top of sample. The furnace was opened to remove excess material. Dynamic viscosity was measured with increasing frequency of 0.1–100 rad/sec. For each frequency sweeps, the linear viscoelastic limits were determined prior to analysis, and the rheological analyses were performed in triplicate.

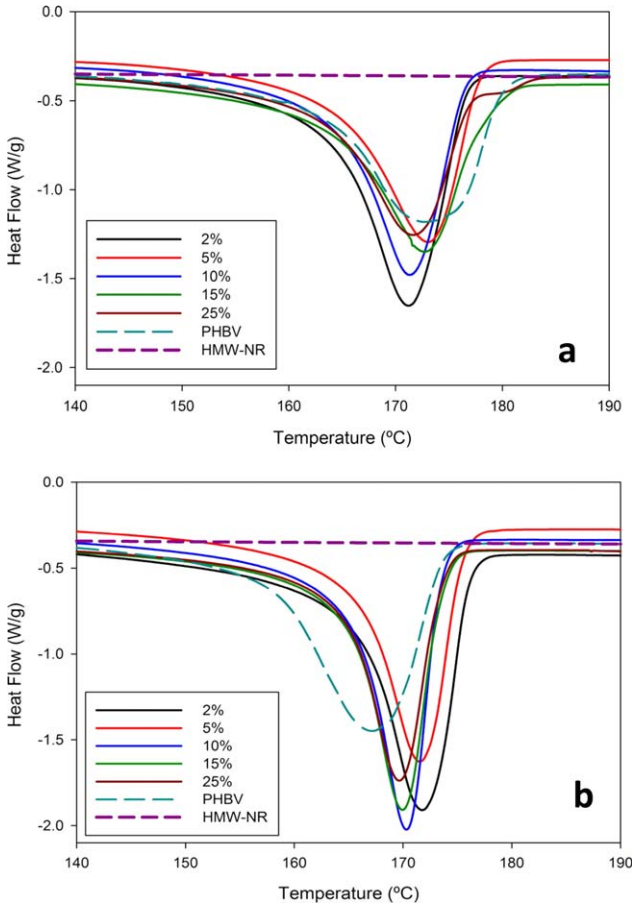

Figure 1. DSC first melting (a) and second melting (b) transitions of blends with pure PHBV and HMW-NR at 10 °C/min. [Color figure can be viewed in the online issue, which is available at wileyonlinelibrary.com.]

RESULTS AND DISCUSSION

Thermal Transitions of Blends

During the first melting scans [Figure 1(a)], the melting temperatures of the blends (170–173 °C) resembled that of pure PHBV (171 °C), except for 2% blend, which showed a broader melting temperature. When the first heating runs were compared with rescanned thermograms [Figure 1(b)], the observed melting was more consistent with a single phase material. The second melting peaks of the blends were sharper compared with the pure PHBV. The peak melting temperatures of the blends in the second melting (170–172 °C) showed minimal change from the first melting, while pure PHBV showed a small decrease (6 °C). The rubber showed no melting transitions, as expected for an amorphous material.

These results differ from those previously published of PHBV blends with butadiene, epoxidized NR, ethylene-vinyl acetate,

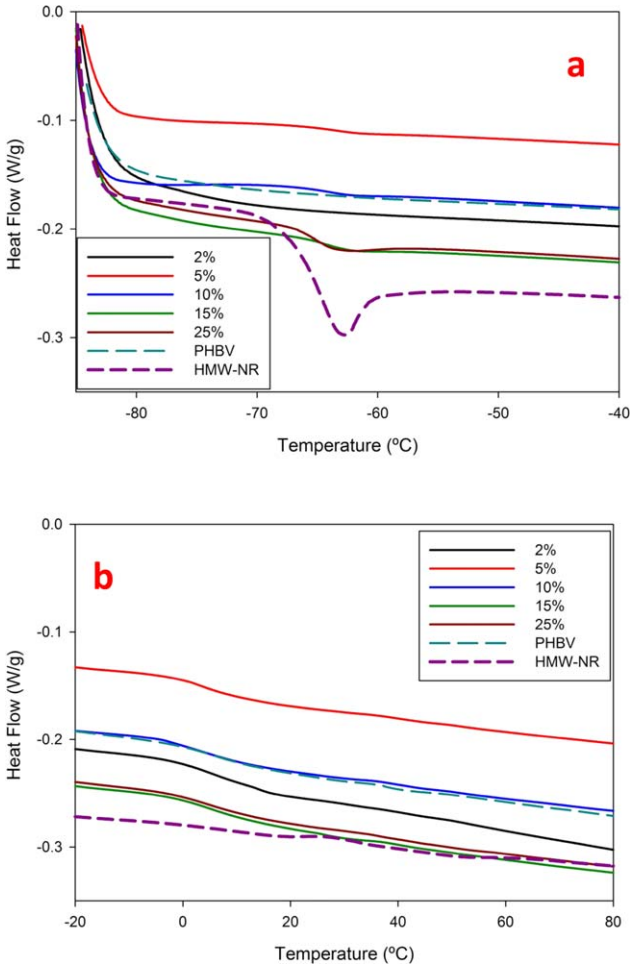

Figure 2. DSC glass transition from second scan of blends and pure HMW-NR (a) and PHBV (b). [Color figure can be viewed in the online issue, which is available at wileyonlinelibrary.com.]

and other rubbers showing two melting peaks attributed to different crystals (PHB and PHV) formed during the annealing phases.[18,25] The uniform melting peaks observed in the current study can be attributed to the HMW-NR, because NR is known to dissipate heat during thermal stress. Thus the better dispersion of heat protected the PHBV from degrading during the heating and rotational stresses of extrusion and injection molding. Similar uniform melting peaks were obtained in blends of medium chain length PHA with nitrile and NR due to the rubber changing the crystallization and melting properties of the PHA.[26] It is also possible that the uniform melting peaks could be due to annealing increasing the compatibility between PHBV and rubber.[22] It has been suggested that the melt reactions that occur during the compounding process begin with scission of long chain PHB molecules to shorter molecules containing carboxyl ends groups.[10–12,22] Subsequently, the ring opening of the epoxide group on the NR allows the reactive carboxyl end groups to bind to the NR.[22] The second heating cycle was used to determine glass transition temperatures (T_g) commonly used to establish miscibility in polymer/polymer blends (Figure 2). All the samples displayed two glass transition temperatures near −65 and −1.0 °C: a miscible polymer blend will exhibit a single T_g. When these thermal properties (T_g and T_m) were compared with traditional thermoplastics, polypropylene (0 and 176 °C) was most similar, while poly(ethylene terephthalate) (PET, 73–80 and 245–265 °C), polystyrene (PS, 70–80 and 100 °C), low-density polyethylene (LDPE, −100 and 95–110 °C) differed significantly.[27,28]

Decomposition of Blends

Thermogravimetric analysis was used to determine the decomposition temperatures for the blends and pure materials due to thermal stress, which are related to the composites losing their functionality as a packaging material (Figure 3). The thermal onset and peak degradation temperatures for pure PHBV were 238 and 288 °C, respectively, and for HMW-NR were 341 and 365 °C. Two stages of weight loss were observed for the blends in the TGA. Within the temperature range 270–293 °C, the thermal onset temperature of the blends resembled that of PHBV. However, at the higher temperature of 270–293 °C, the blends' degradation profiles resembled that of HMW-NR. The onset degradation temperature was 13–23% higher for the blends than for pure PHBV. In addition, the slope of the falling region of the blend reflecting the rate of degradation had a sharper

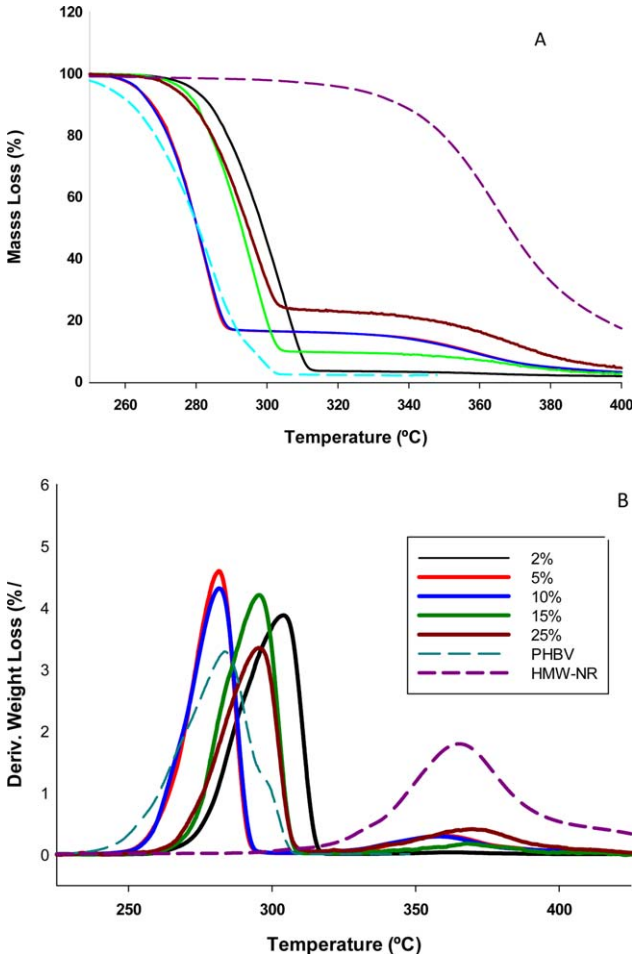

Figure 3. (A) Weight loss TGA thermograms. (B) Derivative weight loss TGA thermograms of blends with pure PHBV and HMW-NR obtained from TGA. [Color figure can be viewed in the online issue, which is available at wileyonlinelibrary.com.]

Table I. Water Vapor Transmission Rates of PHBV, HMW-NR, and Blends ($n = 5$)

PHBV/HMW-NR	Trans. rate (g/[m^2 day])
98/2	29.5 (±17.4)
95/5	34.3 (±2.29)
90/10	15.8 (±1.05)
85/15	6.28 (±1.56)
75/25	3.54 (±0.339)
PHBV	44.3 (±2.98)
HMW-NR	4.34 (±1.13)

slope than pure PHBV. Similar results have been reported for NR, where thermal degradation began at 290 °C with peak degradation at 360 °C.[29,30] No thermal depolymerization occurred below 250 °C, but about 85% of the material degraded between 250 and 400 °C.[29,30] Madorsky and co-workers reported that the thermal degradation of NR between 287 and 400 °C yields 39.0% isoprene, 1.32% dependentene, and small amounts of p-menthene.[29–32] Furthermore, the degradation pattern can be used to calculate the percentage of PHBV to HMW-NR compositions in the blends. The % loss at the maximum degradation temperature of the PHBV and HMW-NR fractions tested accounted for nearly 100% indicating that the blends were properly mixed during the compounding stage.

Water Vapor Transmission of Blends

NR is a hydrophobic hydro-carbon, and has a very low water vapor transmission rate. The average water vapor transmission rates (WVTR) ranged from 44.3 to 4.34 g/m^{-2} day for pure materials and the blends (Table I). With the addition of HMW-NR, water permeation decreased due to the steric hindrance caused by the consequential grafting of PHB chains on to the rubber backbone. Steric hindrance decreases chain flexibility, which prevents the polymer chains from sliding past one another which would decrease the free volume and limit migration of water molecules through the blended material. The HMW-NR is partially crosslinked leading to the same decrease in water permeation. When the results of the WVTR are compared with traditional thermoplastics used in packaging, the WVTR measured in this study are similar to PET (3.48 g/m^{-2} day), oriented polystyrene (OPS, 5.18 g/m^{-2} day), and LDPE (7.90 g/m^{-2} day).[33–35]

Mechanical Properties of Blends: Rheology

The visco-elastic properties of the blends were probed at different temperatures to assess the rheological changes upon HMW-NR addition to PHBV. Representative sweeps of complex viscosity versus frequency at 160–180 °C for PHBV and the blends (Figure 4) indicated that, in general, viscosity decreased with increasing frequency. This is likely due to breakdown of entanglements between the polymer and rubber matrix. All the samples exhibited the shear-thinning behavior typical for non-Newtonian fluids, such as polymer melts. To assess this behavior more quantitatively, the rheological data were fitted to the Power–law or Ostwald–de Waele model, which describes viscosity as a function proportional to some power of the shear rate. The relationship between steady shear and dynamic shear viscosity has been established using the Cox–Merz rule, which holds true for PHA, PHB, and PHBV.[12,36] By substituting the steady shear terms with dynamic viscosity terms, a modified Power-law model is obtained that is expressed as:

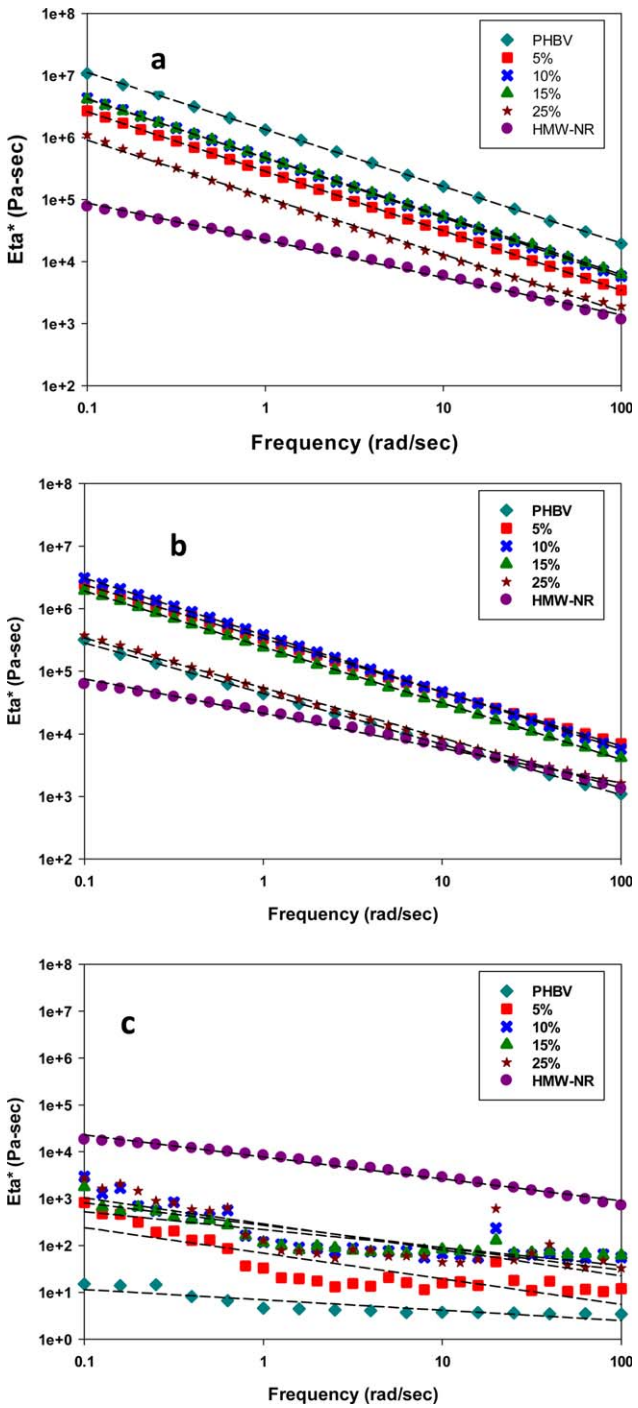

Figure 4. Representative complex viscosity curves of various blends as a function of oscillatory shear frequency and the Power–law data fit curves. $a = 160$ °C, $b = 170$ °C, and $c = 180$ °C. [Color figure can be viewed in the online issue, which is available at wileyonlinelibrary.com.]

Table II. Power–Law Parameters for Pure PHBV and the Blends at 160 °C

PHBV/HMW-NR	Consistency index (Pa s)	Flow behavior index
100/0	1.35×10^6	0.0823
95/5	2.87×10^5	0.0385
90/10	4.67×10^5	0.0410
85/15	4.75×10^5	0.0562
75/25	1.09×10^5	0.0770
0/100	2.21×10^4	0.398

$$|\eta * (\omega)| = m(\omega)^{n-1} \quad (1)$$

The modified model has two parameters that must be fitted to experimental data. The first parameter m, also known as consistency index, is the y-intercept of the log η^* and ω curve. [37] In addition, the consistency index is related to the magnitude of the viscosity in Pa s. The second parameter is the exponent of ω, $n-1$, which is the slope of the log η^* and ω curve and is dimensionless.[37] In the case of shear thinning, the exponent is less than one ($n<1$), and the plot of log η^* and log ω has a negative slope.[37] The consistency index and flow behavior index parameters for pure PHBV and the blends are summarized in Table II and Figure 4(a–c). The consistency index ranged from 2.21×10^4 to 1.35×10^6 Pa s with the lower values being similar to those found for high density poly ethylene. The flow behavior index ranged from 0.0385 to 0.398 for the blends at 160 °C suggesting pseudo-plastic behavior since values were below 1.

The Power–law model fit the data well, with the low to middle frequency range for the 75/25 blends at 160 °C being the only exception [Figure 4(a)]. At 160 °C, pure PHBV had the highest viscosity throughout the frequency range, viscosity decreased with increasing HMW-NR loading in the blends [Figure 4(a)], and pure HMW-NR had lowest viscosity at 160 °C. In contrast, at 170 °C, although the pure HMW-NR was still the least viscous, the viscosities of 95/5, 90/10, and 85/15 blends where higher than at 160 °C, and all blends exhibited higher complex viscosity than pure PHBV [Figure 4(b)]. At 180 °C, only the pure HMW-NR had a viscosity curve similar to that in the two cooler temperatures [Figure 4(a–c)]. The pure PHBV became fluid at 180 °C, which is to be expected since its melt temperature is 171 °C.[10–12] The viscosities of the blends also declined due to the PHBV phase melting and disrupting the blended material structure. The Power–law model was unable to fit the data at 180 °C due to low complex viscosity and fluctuations throughout the frequency range. The relatively constant viscosity of the HMW-NR from 160 to 180 °C, and across the frequency range, appears to provide some stability to the PHBV portion of the blended materials [Figure 4(a–c)].

The storage or elastic modulus, G' (ω), is related to the load bearing capacity or the ability to absorb and store energy of a material, while the loss or viscous modulus, G'' (ω), is the material's ability to dissipate mechanical energy and is proportional to viscous behavior of the material. Both these moduli for the blends and pure materials were obtained from dynamic oscillatory shear at 160–180 °C (data not shown). At the testing temperatures of 160 and 170 °C, the blends, HMW-NR, and PHBV behaved as solid materials. The storage modulus for PHBV and the blends was frequency-independent at 160 °C, and only small frequency-induced changes were apparent at 170 °C. However, the storage modulus for HMW-NR was strongly frequency dependent at 170 and 180 °C, indicating that the blends behaved more like PHBV than HMW-NR at these temperatures. The blends and pure PHBV exhibited higher loss modulus compared with storage modulus throughout the frequency range at 180 °C indicating a liquid-like structure. This coincides with the thermal analysis of these materials, which indicated a melting temperature range from 165 to 173 °C. In contrast, the HMW-NR materials exhibited higher storage modulus compared loss modulus, which is expected from the amorphous and partial crosslinked material. Amorphous materials do not exhibit a well-defined melting point compared with crystalline materials (PHA, PHB, and PHBV), but tend to soften slowly over a wide temperature range which could explain why the complex viscosity was higher for the blends at 170 and 180 °C [Figure 4(b,c)].

Mechanical Properties of Blends: Visco-Elastic Properties

Dynamic mechanical analysis (DMA) was used to characterize the visco-elastic transition at 1 Hz of the PHBV/HMW-NR blends from a brittle to a rubbery state by observing the changes in storage modulus (E') as described elsewhere.[10,38] Storage moduli transitions onset and midpoint temperatures were observed between −61.0 to −45.0 °C and 7.27 to 38.0 °C for the PHBV/HMW-NR blends and pure PHBV (Figure 5). Similar to conventional thermoplastics, E' decreased significantly with increasing temperature.[10,38] The 95/5 blends had the highest storage modulus of all the blends, and the modulus decreased with increasing HMW-NR loadings, as expected since HMW-NR has a lower E' than PHBV. This is further illustrated by the 52% lower modulus in the 75/25 blend compared with the 95/5 blend observed during the PHBV glass transition (3537 ± 2754 and 7399 ± 1770, respectively).

Tan delta (δ) is the ratio of loss modulus (E'') to storage modulus (E'), and is used to express the energy dissipated as heat

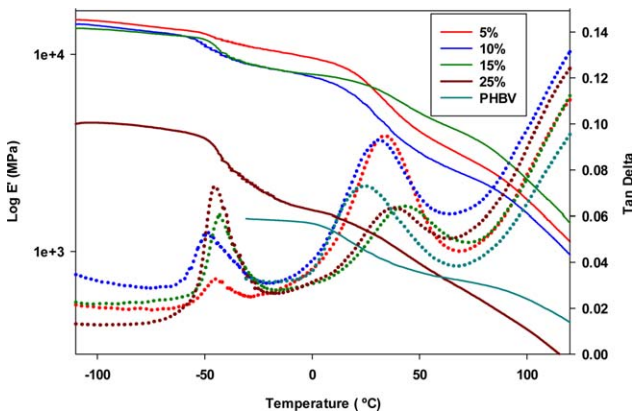

Figure 5. Storage modulus (E', solid lines) and Tan Delta (δ, dotted lines) for pure PHBV and blends during temperature sweeps at 5 °C/min obtained via DMA. [Color figure can be viewed in the online issue, which is available at wileyonlinelibrary.com.]

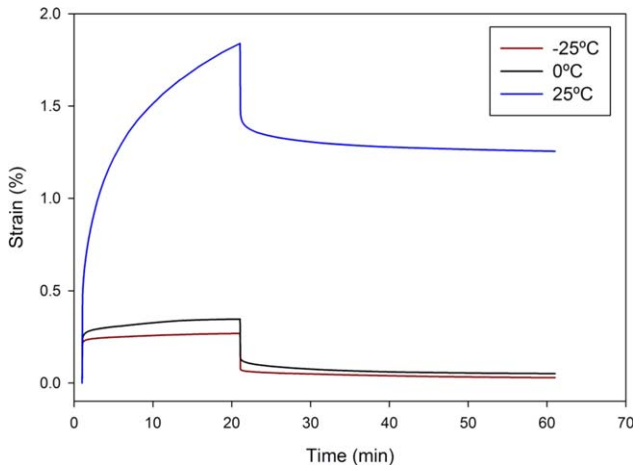

Figure 6. Effect of temperature on creep and recovery strain (%) of 90/10 PHBV/HMW-NR blends. [Color figure can be viewed in the online issue, which is available at wileyonlinelibrary.com.]

during the heating cycle (Figure 5). The damping peaks occurred between −50 to −40 °C and 30 to 40 °C for the HMW-NR and PHBV components of the blends, respectively (Figure 5). The higher HMW-NR contents of 15 and 25% resulted in higher amplitude of the tan delta peaks, which suggests increased mobility of the rubber near −50 °C. The rubber polymer chains in 5 and 10% HMW-NR appeared to have more limited mobility, and the damping was lower as the properties of the PHBV became more predominant. PHBV is stiff and brittle at −50 °C. However, the inverse response was observed near the PHBV glass transition (30 °C), where blends with only 5 and 10% HMW-NR exhibited higher dampening and more chain flexibility compared with blends with 15 and 25% HMW-NR. The addition of HMW-NR markedly increased the temperature at which the PHBV tan delta in the blends reached a maximum, indicating intimate interactions between the rubber component and the PHBV matrix.

Creep is a progressive deformation of a material under constant stress, while recovery is the measurement of the material response after the constant stress is removed. The maximum creep increased with temperature due to softening of the polymer (Figure 6). The % creep strain increased with temperature because of increased chain mobility due to reduced entanglement of the molecular chains as the material transitioned from the brittle state (−25 and 0 °C) to a more flexible state (25 °C) (Figure 6, Table III). Similar trends in the creep compliances and recovery were observed with all PHBV/HMW-NR blends. The change in the sample state would also explain why the elastic recovery is higher than the viscous recovery (Table III). The recovery decreased with loading due to more chain entanglement, which prevented the chains from disentangling. The creep and recovery compliances increased with rubber loading due to the rubber matrix being less resistant to creep than the PHBV, while the recovery compliance increased because reformation rapidly occurs for partially crosslinked materials like HMW-NR. In addition, the higher compliance values of the blends suggest a high entanglement network of PHBV and rubber micro-fibrils. This entanglement network stabilized the blends and prevented permanent structural damage after the initial elastic deformation.

The stress–strain behavior of PHBV was typical of a brittle polymer.[10,12] The material extended or stretched linearly up to a strain of 1% due to its glass-transition temperature (7.37–21.5 °C) being close to the testing temperature (26 °C). The failure at low strains has been attributed to spherulites in the amorphous phase inhibiting flow of the crystallite region.[12,17] The incorporation of HMW-NR into PHBV increased the elongation at break, but decreased the tensile strength (Table IV). These effects were more pronounced the greater the proportion of HMW-NR in the blend. The elongation at break increased by approximately 32% with the addition of 25% rubber compared with pure PHBV (Table IV) likely due to the integral blending of the rubber and the PHBV matrix.[17] In the same blends, this increase was accompanied by a decrease of tensile strength attributed to the increasing loading of the rubber, which causes weaker interfacial areas between the elastomer and the polymer matrix.[17,39] However, despite these changes, the blends retained considerable tensile strength, adequate for many applications.

Rubber addition lowered the modulus of PHBV by 19–30%.[17,39] However, in our HMW-NR/PHBV blends, the Young's modulus was not significantly altered compared with PHBV alone suggesting that the PHBV phase was predominant, but the variation in modulus among samples within each material was high (Table IV). The elastic moduli of the HMW-NR/PHBV blends (5.26–10.3 GPa) were higher than those of traditional

Table III. Creep and recovery results of 90/10 and 75/25 blends at three temperatures (−25, 0, and 25 °C)

	Max. creep (%)	Elastic recovery (%)	Viscous recovery (%)	Creep compliance (Pa^{-1})	Recovery compliance (Pa^{-1})
90/10					
−25 °C	29.8 (±14.8)	95.4 (±5.66)	8.49 (±2.29)	392 (±10.7)	371 (±89.1)
0 °C	58.4 (±6.51)	78.6 (±16.2)	21.4 (±16.2)	817 (±46.4)	567 (±207)
25 °C	373 (±37.5)	29.6 (±2.16)	59.7 (±12.8)	2793 (±884)	847 (±321)
75/25					
−25 °C	52.8 (±2.17)	86.8 (±4.68)	12.9 (±5.00)	357 (±10.7)	321 (±26.2)
0 °C	60.8 (±8.93)	79.0 (±1.20)	18.8 (2.67)	935 (±279)	736 (±213)
25 °C	191 (±23.3)	52.8 (±5.87)	47.3 (5.87)	5979 (±417)	1242 (±136)

Table IV. Mechanical Properties of Pure PHBV and the Blends (Different Letters Reflect P Values < 0.05)

PHBV/HMW-NR	Elongation at break (%)	Tensile strength (MPa)	Young's modulus (GPa)	HDT (°C)
100/0	1.39^{a,b} (±0.14)	35.6^{a} (±1.72)	8.05^{a,b} (±5.67)	145^{a} (±0.74)
95/5	1.56^{b,c} (±0.16)	28.2^{b} (±4.79)	8.96^{a,b} (±5.43)	145^{a} (±2.66)
90/10	1.51^{a,b,c} (±0.24)	22.1^{c} (±1.87)	5.26^{a} (±1.77)	142^{a} (±8.71)
85/15	1.20^{c} (±0.22)	22.7^{c} (±1.40)	8.54^{b} (±1.37)	129^{a,b} (±7.52)
75/25	1.84^{c} (±0.59)	19.1^{d} (±1.12)	9.89^{a,b} (±5.89)	122^{b} (±5.46)

thermoplastics, such as low-density polyethylene (LDPE, 0.2 GPa), poly(ethylene terephthalate) (PET, 2.8–4.1 GPa), polypropylene (PP, 1.7 GPa), and polystyrene (PS, 2.3–3.3 GPa).[26,40] However, these plastics can absorb higher strain before breaking as measured by percent elongation at break. The blends had much lower elongation at break value of 1.20–1.84% compared with PET (30–300%), PS (2.50%), LDPE (100–1000%), and PP (400%).[27,28] Finally, the blends had similar tensile strength value (22.1–35.0 MPa) to LDPE (8–20 MPa), PS (34–50 MPa), and PP (38 MPa), although, as is well known, PHBV alone is much stronger (48–72 MPa).[27,40]

Mechanical Properties of Blends: Heat Deflection Temperature

The heat deflection temperature (HDT) is the temperature at which a sample deforms under a specific, or normal, load. Below the HDT, the sample retains its shape under its normal load. Above the HDT the sample is beyond its usable temperature range. HDT is greatly affected by the glass transition (T_g) and crystallinity of the material. The HDT of an amorphous material, like HMW-NR, is near its T_g (−60 °C) while that of a semi-crystalline material, like PHBV, is near its melting temperature.[41] Increasing HMW-NR content decreased HDT in the blends (Table III), most pronounced in 25% HMW-NR. When the HDT of the HMW-NR/PHBV blends was compared with traditional plastics, they had higher HDT's (122–145 °C) than PE (85 °C), PET (70 °C), PP (100 °C), and PS (95 °C).[42]

CONCLUSIONS

The addition of HMW-NR to PHBV improved the elongation to break properties of the blends, while the thermal data suggest potential grafting of the of the PHBV polymer onto the rubber backbone. The blends had higher complex viscosity compared with pure PHBV due to better heat dispersion mediated by the rubber component in the blends. The improved dispersion of heat may prevent the PHBV blends from degrading during heating and rotational stresses of injection molding. The blends combined the visco-elastic properties of the elastomeric and thermoplastic materials. The rubber provided elastomeric properties at the lower temperature of storage (−25 °C), while the thermoplastic provided the structural rigidity needed at the higher melting temperatures. Furthermore, the blends had better water resistance than PHBV that can aid in certain applications. Thus, these bio-plastic and rubber blends may replace petroleum-derived packaging, while providing equivalent functionality and properties. Some commercial applications for 5 and 10% blends would include plastic lids for cups (*Candy, species lids, blender lids are some examples*). These blends show greater chain flexibility at room temperature, which would allow the molecular chains to offset the compressive force needed to close the lid. During the creep and recovery testing, all the blends exhibit higher recover compliance suggesting reformation and realignment of the blends to offset the compressive force. Based on the lower WVTR, these blends could replace traditional thermoplastic that require low moisture barrier and flavor migration like multilaminated wrappers.

ACKNOWLEDGMENTS

This work was supported by an Ohio Agricultural Research and Development Center and Center for Advanced Processing and Packaging Studies (CAPPS) grants. Furthermore, the authors would like to thank The Ohio BioProducts Innovation Center (OBIC) for supplying the instruments used in this study, and Dr. Jose Castro and Eusebio Cabrera for assisting with the injection molding of the composites. Authors would also like to acknowledge USDA National Institute of Food and Agriculture (Hatch project 230837).

REFERENCES

1. http://www.plasticseurope.org/documents/document/20121120170458-final_plasticsthefacts_nov2012_en_web_resolution.pdf [Accessed on May 18, **2014**].
2. El-Hadi, A.; Schnabel, R.; Straube, E.; Muller, G.; Riemschneider, M. *Macromol. Mater. Eng.* **2002**, *287*, 363.
3. Holmes, P. A. Biologically Produced (R)−3-Hydroxyalkanoate Polymers and Copolymers; Elsevier: London, **1998**.
4. http://www.epa.gov/waste/nonhaz/municipal/ [Accessed on May 18, **2014**].
5. Ferreira, B. M. P.; Zavaglia, C.; Duek, E. *J. Appl. Polym. Sci.* **2002**, *86*, 2898.
6. Ramkumar, D.; Bhattacharya, M. *Polym. Eng. Sci.* **2004**, *38*, 1426.
7. Verhoogt, H.; Ramsay, B.; Favis, B.; Ramsay, J. *J. Appl. Polym. Sci.* **1996**, *61*, 87.
8. Wang, S.; Ma, P.; Wang, R.; Wang, S.; Zhang, Y. *J. Polym. Degrad. Stabil.* **2008**, *93*, 1364.
9. Marcilla, A.; Garcia-Quesada, C.; Lopez, M.; Gil, E. *J. Appl. Polym. Sci.* **2009**, *113*, 3187.
10. Modi, S.; Koelling, K.; Vodovotz, Y. *Eur. Polym. J.* **2011**, *47*, 179.
11. Modi, S.; Koelling, K.; Vodovotz, Y. *J. Appl. Polym. Sci.* **2012**, *124*, 3074.

12. Modi, S.; Koelling, K.; Vodovotz, Y. *Eur. Polym. J.* **2013**, *43*, 3681.
13. Sethuraj, M. R.; Mathew, N. T., Ed. In Developments in Crop Science 23 Natural Rubber: Biology, Cultivation and Technology; Elsevier: London, **1992**.
14. Venkatachalam, R.; Geetha, N.; Sangeetha, P.; Thulaseedharan, *Afr. J. Biotechnol.* **2013**, *12*, 1297.
15. Aguel, F; Madufor, C. *J. Polym. Sci.* **2012**;*2*(3):28; Biosynthesis of Natural Rubber and Other Natural Polyisoprenoids. Biopolymer. Wiley: New York, 2001; p 75.
16. Cain, M. Engineering Design with Natural Fiber; Malaysian Rubber Producers' Research Association: Hertford, England.
17. Abbate, M.; Martuscelli, E.; Rogosta, G.; Carinzi, G. *J. Mater. Sci.* **1991**, *26*, 1119.
18. Parulekar, Y.; Mohanty, A. *Green Chem.* **2005**, *8*, 206.
19. Sadocco, P.; Canetti, M.; Seves, A. *Polymer* **1993**, *34*, 3368.
20. Martuscelli, E.; Maurizio, A. *Polymer* **1988**, *29*, 1731.
21. Maurizio, A.; Martuscelli, E.; Greco, P. *Polymer* **1991**, *32*, 1647.
22. Lee, H. K.; Ismail, J.; Krammer, H. W.; Bakar, M. A. *J. Appl. Polym. Sci.* **2005**, *95*, 113.
23. Sadocco, P.; Bulli, C.; Elegir, G.; Seves, A. *Macromol. Chem.* **1993**, *194*, 2675.
24. Modi, S.; Cornish, K.; Koelling, K.; Vodovotz, Y. SPE ANTEC **2014**; p 330.
25. Yoon, J.; Oh, S.; Kim, M. *Polymer* **1998**, *39*, 2479.
26. Bhatt, R.; Shah, D.; Patel, K. C.; Trivedi, U. *Bioresour. Technol.* **2008**, *99*, 4615.
27. Sudesh, K.; Doi, K. *Prog. Polym. Sci.* **2000**, *25*, 1503.
28. Clarinval, A.; Halleux, J. In Classification of Biodegradable Polymers; Smith, R., Ed.; Woodhead Publishing Ltd: Cambridge, UK, **2005**; p 3.
29. Mathew, A.; Packirisamy, S.; Thomas, S. *J. Polym. Degrad. Stabil.* **2001**, *72*, 423.
30. Ramesan, M. T. *React. Funct. Polym.* **2004**, *59*, 267.
31. Straus, S.; Madorsky, S. L. *J. Res. Natl. Bur. Stand.* **1953**, *50*, 165.
32. Madorsky, S. L.; Straus, S.; Thompson, D.; Williamson, L. *J. Res. Natl. Bur. Stand.* **1949**, *42*, 499.
33. Auras, R.; Singh, S.; Singh, J. *Packag. Technol. Sci.* **2005**, *18*, 207.
34. Jagannath, J.; Nadanasbapathi, S.; Bawa, A. J. *J. Appl. Polym. Sci.* **2006**, *99*, 3355.
35. Plackett, D.; Holm, V.; Johansen, P.; Ndoni, S. *Packag. Technol. Sci.* **2006**, *19*, 1.
36. Liao, Q.; Noda, I.; Frank, C. *Polymer* **2009**, *50*, 6139.
37. Morrison, F. Understanding Rheology; New York: Oxford University Press, **2001**.
38. Singh, S.; Mohanty, A.; Sugie, T.; Takai, Y.; Hamada, H. *Compos. Part A* **2008**, *39*, 875.
39. Calvao, P.; Chenal, J.; Gauthier, C.; Demarquette, N.; Bogner, A.; Cavaille, J. *Polym. Int.* **2012**, *61*, 434.
40. Clarinval, A.; Halleux, J. In Classification of Biodegradable Polymers; Smith, R., Ed.; Woodhead Publishing Ltd.: Cambridge, UK, **2005**; p 3.
41. Kawamoto, N.; Sakai, A.; Horikoshi, T.; Urushihara, T.; Tobita, E. *J. Appl. Polym. Sci.* **2007**, *103*, 244.
42. Mckeen, L.; Andrew, W. Ed. In Plastics Design Library Effect of Temperature and Other Factors on Plastics and Elastomers; William Andrew: Oxford, **2014**; p 649.